

<sup>1</sup> **Critical transitions and the fragmenting of global forests**

<sup>2</sup> **Leonardo A. Saravia<sup>1 3</sup>, Santiago R. Doyle<sup>1</sup>, Benjamin Bond-Lamberty<sup>2</sup>**

<sup>3</sup> 1. Instituto de Ciencias, Universidad Nacional de General Sarmiento, J.M. Gutierrez 1159 (1613), Los  
<sup>4</sup> Polvorines, Buenos Aires, Argentina.

<sup>5</sup> 2. Pacific Northwest National Laboratory, Joint Global Change Research Institute at the University of  
<sup>6</sup> Maryland–College Park, 5825 University Research Court #3500, College Park, MD 20740, USA

<sup>7</sup> 3. Corresponding author e-mail: lsaravia@ungs.edu.ar

<sup>8</sup> **keywords:** Forest fragmentation, early warning signals, percolation, power-laws, MODIS, critical transitions

<sup>9</sup> **Running title:** Critical fragmentation in global forest

<sup>10</sup> **Abstract**

<sup>11</sup> 1. Forests provide critical habitat for many species, essential ecosystem services, and are coupled to  
<sup>12</sup> atmospheric dynamics through exchanges of energy, water and gases. One of the most important  
<sup>13</sup> changes produced in the biosphere is the replacement of forest areas with human dominated landscapes.  
<sup>14</sup> This usually leads to fragmentation, altering the sizes of patches, the structure and function of the  
<sup>15</sup> forest. Here we studied the distribution and dynamics of forest patch sizes at a global level, examining  
<sup>16</sup> signals of a critical transition from an unfragmented to a fragmented state.

<sup>17</sup> 2. We used MODIS vegetation continuous field to estimate the forest patches at a global level and de-  
<sup>18</sup> fined wide regions of connected forest across continents and big islands. We search for critical phase  
<sup>19</sup> transitions, where the system state of the forest changes suddenly at a critical point in time; this  
<sup>20</sup> implies an abrupt change in connectivity that causes an increased fragmentation level. We studied the  
<sup>21</sup> distribution of forest patch sizes and the dynamics of the largest patch over the last fourteen years,  
<sup>22</sup> as the conditions that indicate that a region is near a critical fragmentation threshold are related to  
<sup>23</sup> patch size distribution and temporal fluctuations of the largest patch.

<sup>24</sup> 3. We found some evidence that allows us to analyze fragmentation as a critical transition: most regions  
<sup>25</sup> followed a power-law distribution over the 14 years. We also found that the Philippines region probably  
<sup>26</sup> went through a critical transition from a fragmented to an unfragmented state. Only the tropical forest  
<sup>27</sup> of Africa and South America met the criteria to be near a critical fragmentation threshold.

28     4. This implies that human pressures and climate forcings might trigger undesired effects of fragmentation,  
29       such as species loss and degradation of ecosystems services, in these regions. The simple criteria  
30       proposed here could be used as an early warning to estimate the distance to a fragmentation threshold  
31       in forest around the globe and a predictor of a planetary tipping point.

## **32    Introduction**

33    Forests are one of the most important biomes on earth, providing habitat for a large proportion of species  
34    and contributing extensively to global biodiversity (Crowther *et al.* 2015). In the previous century human  
35    activities have influenced global bio-geochemical cycles (Bonan 2008; Canfield, Glazer & Falkowski 2010),  
36    with one of the most dramatic changes being the replacement of 40% of Earth's formerly biodiverse land  
37    areas with landscapes that contain only a few species of crop plants, domestic animals and humans (Foley  
38    *et al.* 2011). These local changes have accumulated over time and now constitute a global forcing (Barnosky  
39    *et al.* 2012).

40    Another global scale forcing that is tied to habitat destruction is fragmentation, which is defined as the  
41    division of a continuous habitat into separated portions that are smaller and more isolated. Fragmentation  
42    produces multiple interwoven effects: reductions of biodiversity between 13% and 75%, decreasing forest  
43    biomass, and changes in nutrient cycling (Haddad *et al.* 2015). The effects of fragmentation are not only  
44    important from an ecological point of view but also that of human activities, as ecosystem services are deeply  
45    influenced by the level of landscape fragmentation (Mitchell *et al.* 2015).

46    Ecosystems have complex interactions between species and present feedbacks at different levels of organization  
47    (Gilman *et al.* 2010), and external forcings can produce abrupt changes from one state to another, called  
48    critical transitions (Scheffer *et al.* 2009). These abrupt state shifts cannot be linearly forecasted from past  
49    changes, and are thus difficult to predict and manage (Scheffer *et al.* 2009). Such 'critical' transitions have  
50    been detected mostly at local scales (Drake & Griffen 2010; Carpenter *et al.* 2011), but the accumulation of  
51    changes in local communities that overlap geographically can propagate and theoretically cause an abrupt  
52    change of the entire system at larger scales (Barnosky *et al.* 2012). Coupled with the existence of global  
53    scale forcings, this implies the possibility that a critical transition could occur at a global scale (Rockstrom  
54    *et al.* 2009; Folke *et al.* 2011).

55    Complex systems can experience two general classes of critical transitions (Solé 2011). In so-called first  
56    order transitions, a catastrophic regime shift that is mostly irreversible occurs because of the existence of  
57    alternative stable states (Scheffer *et al.* 2001). This class of transitions is suspected to be present in a variety  
58    of ecosystems such as lakes, woodlands, coral reefs (Scheffer *et al.* 2001), semi-arid grasslands (Bestelmeyer  
59    *et al.* 2011), and fish populations (Vasilakopoulos & Marshall 2015). They can be the result of positive  
60    feedback mechanisms (Martín *et al.* 2015); for example, fires in some forest ecosystems were more likely to  
61    occur in previously burned areas than in unburned places (Kitzberger *et al.* 2012).

62    The other class of critical transitions are continuous or second order transitions (Solé & Bascompte 2006).

63 In these cases, there is a narrow region where the system suddenly changes from one domain to another,  
64 with the change being continuous and in theory reversible. This kind of transitions were suggested to be  
65 present in tropical forest (Pueyo *et al.* 2010), semi-arid mountain ecosystems (McKenzie & Kennedy 2012),  
66 tundra shrublands (Naito & Cairns 2015). The transition happens at a critical point where we can observe a  
67 distinctive spatial pattern: scale invariant fractal structures characterized by power law patch distributions  
68 (Stauffer & Aharony 1994).

69 There are several processes that can convert a catastrophic transition to a second order transitions (Martín  
70 *et al.* 2015). These include stochasticity, such as demographic fluctuations, spatial heterogeneities, and/or  
71 dispersal limitation. All these components are present in forest around the globe (Seidler & Plotkin 2006;  
72 Filotas *et al.* 2014; Fung *et al.* 2016), and thus continuous transitions might be more probable than  
73 catastrophic transitions. Moreover there is some evidence of recovery in some systems that supposedly  
74 suffered an irreversible transition produced by overgrazing (Zhang *et al.* 2005) and desertification (Allington  
75 & Valone 2010).

76 The spatial phenomena observed in continuous critical transitions deal with connectivity, a fundamental  
77 property of general systems and ecosystems from forests (Ochoa-Quintero *et al.* 2015) to marine ecosystems  
78 (Leibold & Norberg 2004) and the whole biosphere (Lenton & Williams 2013). When a system goes from a  
79 fragmented to a connected state we say that it percolates (Solé 2011). Percolation implies that there is a  
80 path of connections that involves the whole system. Thus we can characterize two domains or phases: one  
81 dominated by short-range interactions where information cannot spread, and another in which long range  
82 interactions are possible and information can spread over the whole area. (The term “information” is used  
83 in a broad sense and can represent species dispersal or movement.)

84 Thus, there is a critical “percolation threshold” between the two phases, and the system could be driven  
85 close to or beyond this point by an external force; climate change and deforestation are the main forces  
86 that could be the drivers of such a phase change in contemporary forests (Bonan 2008; Haddad *et al.* 2015).  
87 There are several applications of this concept in ecology: species’ dispersal strategies are influenced by  
88 percolation thresholds in three-dimensional forest structure (Solé, Bartumeus & Gamarra 2005), and it has  
89 been shown that species distributions also have percolation thresholds (He & Hubbell 2003). This implies  
90 that pushing the system below the percolation threshold could produce a biodiversity collapse (Bascompte  
91 & Solé 1996; Solé, Alonso & Saldaña 2004; Pardini *et al.* 2010); conversely, being in a connected state (above  
92 the threshold) could accelerate the invasion of forest into prairie (Loehle, Li & Sundell 1996; Naito & Cairns  
93 2015).

94 One of the main challenges with systems that can experience critical transitions—of any kind—is that the  
95 value of the critical threshold is not known in advance. In addition, because near the critical point a small  
96 change can precipitate a state shift of the system, they are difficult to predict. Several methods have been  
97 developed to detect if a system is close to the critical point, e.g. a deceleration in recovery from perturbations,  
98 or an increase in variance in the spatial or temporal pattern (Hastings & Wysham 2010; Carpenter *et al.*  
99 2011; Boettiger & Hastings 2012; Dai *et al.* 2012).

100 In this study, our objective is to look for evidence that forests around the globe are near continuous critical  
101 point that represent a fragmentation threshold. We use the framework of percolation to first evaluate if  
102 forest patch distribution at a continental scale is described by a power law distribution and then examine  
103 the fluctuations of the largest patch. The advantage of using data at a continental scale is that for very large  
104 systems the transitions are very sharp (Solé 2011) and thus much easier to detect than at smaller scales,  
105 where noise can mask the signals of the transition.

## 106 Methods

### 107 Study areas definition

108 We analyzed mainland forests at a continental scale, covering the whole globe, by delimiting land areas with  
109 a near-contiguous forest cover, separated with each other by large non-forested areas. Using this criterion,  
110 we delimited the following forest regions. In America, three regions were defined: South America temperate  
111 forest (SAT), subtropical and tropical forest up to Mexico (SAST), and USA and Canada forest (NA). Europe  
112 and North Asia were treated as one region (EUAS). The rest of the delimited regions were South-east Asia  
113 (SEAS), Africa (AF), and Australia (OC). We also included in the analysis islands larger than  $10^5 \text{ km}^2$ . The  
114 mainland region has the number 1 e.g. OC1, and the nearby islands have consecutive numeration (Appendix  
115 S4, figure S1-S6).

### 116 Forest patch distribution

117 We studied forest patch distribution in each defined area from 2000 to 2014 using the MODerate-resolution  
118 Imaging Spectroradiometer (MODIS) Vegetation Continuous Fields (VCF) Tree Cover dataset version 051  
119 (DiMiceli *et al.* 2015). This dataset is produced at a global level with a 231-m resolution, from 2000 onwards  
120 on an annual basis. There are several definition of forest based on percent tree cover (Sexton *et al.* 2015);  
121 we choose a 30% threshold to convert the percentage tree cover to a binary image of forest and non-forest

122 pixels. This was the definition used by the United Nations' International Geosphere-Biosphere Programme  
123 (Belward 1996), and studies of global fragmentation (Haddad *et al.* 2015). This definition avoids the errors  
124 produced by low discrimination of MODIS VCF between forest and dense herbaceous vegetation at low forest  
125 cover (Sexton *et al.* 2015). Patches of contiguous forest were determined in the binary image by grouping  
126 connected forest pixels using a neighborhood of 8 forest units (Moore neighborhood).

## 127 Percolation theory

128 A more in-depth introduction to percolation theory can be found elsewhere (Stauffer & Aharony 1994) and  
129 a review from an ecological point of view is available (Oborny, Szabó & Meszéna 2007). Here, to explain  
130 the basic elements of percolation theory we formulate a simple model: we represent our area of interest by a  
131 square lattice and each site of the lattice can be occupied—e.g. by forest—with a probability  $p$ . The lattice  
132 will be more occupied when  $p$  is greater, but the sites are randomly distributed. We are interested in the  
133 connection between sites, so we define a neighborhood as the eight adjacent sites surrounding any particular  
134 site. The sites that are neighbors of other occupied sites define a patch. When there is a patch that connects  
135 the lattice from opposite sides, it is said that the system percolates. When  $p$  is increased from low values, a  
136 percolating patch suddenly appears at some value of  $p$  called the critical point  $p_c$ .

137 Thus percolation is characterized by two well defined phases: the unconnected phase when  $p < p_c$  (called  
138 subcritical in physics), in which species cannot travel far inside the forest, as it is fragmented; in a general  
139 sense, information cannot spread. The second is the connected phase when  $p > p_c$  (supercritical), species  
140 can move inside a forest patch from side to side of the area (lattice), i.e. information can spread over the  
141 whole area. Near the critical point several scaling laws arise: the structure of the patch that spans the area  
142 is fractal, the size distribution of the patches is power-law, and other quantities also follow power-law scaling  
143 (Stauffer & Aharony 1994).

144 The value of the critical point  $p_c$  depends on the geometry of the lattice and on the definition of the  
145 neighborhood, but other power-law exponents only depend on the lattice dimension. Close to the critical  
146 point, the distribution of patch sizes is:

$$147 (1) n_s(p_c) \propto s^{-\alpha}$$

148 where  $n_s(p)$  is the number of patches of size  $s$ . The exponent  $\alpha$  does not depend on the details of the  
149 model and it is called universal (Stauffer & Aharony 1994). These scaling laws can be applied for landscape  
150 structures that are approximately random, or at least only correlated over short distances (Gastner *et al.*  
151 2009). In physics this is called “isotropic percolation universality class”, and corresponds to an exponent

152  $\alpha = 2.05495$ . If we observe that the patch size distribution has another exponent it will not belong to this  
153 universality class and some other mechanism should be invoked to explain it. Percolation thresholds can also  
154 be generated by models that have some kind of memory (Hinrichsen 2000; Ódor 2004): for example, a patch  
155 that has been exploited for many years will recover differently than a recently deforested forest patch. In  
156 this case, the system could belong to a different universality class, or in some cases there is no universality,  
157 in which case the value of  $\alpha$  will depend on the parameters and details of the model (Corrado, Cherubini &  
158 Pennetta 2014).

159 To illustrate these concepts, we conducted simulations with a simple forest model with only two states: forest  
160 and non-forest. This type of model is called a “contact process” and was introduced for epidemics (Harris  
161 1974), but has many applications in ecology (Solé & Bascompte 2006; Gastner *et al.* 2009). A site with forest  
162 can become extinct with probability  $e$ , and produce another forest site in a neighborhood with probability  
163  $c$ . We use a neighborhood defined by an isotropic power law probability distribution. We defined a single  
164 control parameter as  $\lambda = c/e$  and ran simulations for the subcritical fragmentation state  $\lambda < \lambda_c$ , with  $\lambda = 2$ ,  
165 near the critical point for  $\lambda = 2.5$ , and for the supercritical state with  $\lambda = 5$  (see supplementary data, gif  
166 animations).

## 167 Patch size distributions

168 We fitted the empirical distribution of forest patch areas, based on the MODIS-derived data described above,  
169 to four distributions using maximum likelihood estimation (Goldstein, Morris & Yen 2004; Clauset, Shalizi  
170 & Newman 2009). The distributions were: power-law, power-law with exponential cut-off, log-normal, and  
171 exponential. We assumed that the patch size distribution is a continuous variable that was discretized by  
172 remote sensing data acquisition procedure.

173 We set a minimal patch size ( $X_{min}$ ) at nine pixels to fit the patch size distributions to avoid artifacts at patch  
174 edges due to discretization (Weerman *et al.* 2012). Besides this hard  $X_{min}$  limit we set due to discretization,  
175 the power-law distribution needs a lower bound for its scaling behavior. This lower bound is also estimated  
176 from the data by maximizing the Kolmogorov-Smirnov (KS) statistic, computed by comparing the empirical  
177 and fitted cumulative distribution functions (Clauset *et al.* 2009). We also calculated the uncertainty of the  
178 parameters using a non-parametric bootstrap method (Efron & Tibshirani 1994), and computed corrected  
179 Akaike Information Criteria ( $AIC_c$ ) and Akaike weights for each model (Burnham & Anderson 2002). Akaike  
180 weights ( $w_i$ ) are the weight of evidence in favor of model  $i$  being the actual best model given that one of the  
181  $N$  models must be the best model for that set of  $N$  models.

182 Additionally, we computed the goodness of fit of the power-law model following the bootstrap approach  
183 described by Clauset et. al (2009), where simulated data sets following the fitted model are generated, and a  
184  $p$ -value computed as the proportion of simulated data sets that has a KS statistic less extreme than empirical  
185 data. The criterion to reject the power law model suggested by Clauset et. al (2009) was  $p \leq 0.1$ , but as we  
186 have a very large  $n$ , meaning that negligible small deviations could produce a rejection (Klaus, Yu & Plenz  
187 2011), we chose a  $p \leq 0.05$  to reject the power law model.

188 To test for differences between the fitted power law exponent for each study area we used a generalized least  
189 squares linear model (Zuur *et al.* 2009) with weights and a residual auto-correlation structure. Weights were  
190 the bootstrapped 95% confidence intervals and we added an auto-regressive model of order 1 to the residuals  
191 to account for temporal autocorrelation.

## 192 **Largest patch dynamics**

193 The largest patch is the one that connects the highest number of sites in the area. This has been used  
194 extensively to indicate fragmentation (Gardner & Urban 2007; Ochoa-Quintero *et al.* 2015). The relation of  
195 the size of the largest patch  $S_{max}$  to critical transitions has been extensively studied in relation to percolation  
196 phenomena (Stauffer & Aharony 1994; Bazant 2000; Botet & Ploszajczak 2004), but seldom used in ecological  
197 studies (for an exception see Gastner *et al.* (2009)). When the system is in a connected state ( $p > p_c$ ) the  
198 landscape is almost insensitive to the loss of a small fraction of forest, but close to the critical point a minor  
199 loss can have important effects (Solé & Bascompte 2006; Oborny *et al.* 2007), because at this point the  
200 largest patch will have a filamentary structure, i.e. extended forest areas will be connected by thin threads.  
201 Small losses can thus produce large fluctuations.

202 One way to evaluate the fragmentation of the forest is to calculate the proportion of the largest patch against  
203 the total area (Keitt, Urban & Milne 1997). The total area of the regions we are considering (Appendix S4,  
204 figures S1-S6) may not be the same than the total area that the forest could potentially occupy, thus a more  
205 accurate way to evaluate the weight of  $S_{max}$  is to use the total forest area, that can be easily calculated  
206 summing all the forest pixels. We calculate the proportion of the largest patch for each year, dividing  $S_{max}$   
207 by the total forest area of the same year:  $RS_{max} = S_{max} / \sum_i S_i$ . This has the effect of reducing the  $S_{max}$   
208 fluctuations produced due to environmental or climatic changes influences in total forest area. When the  
209 proportion  $RS_{max}$  is large (more than 60%) the largest patch contains most of the forest so there are fewer  
210 small forest patches and the system is probably in a connected phase. Conversely, when it is low (less than  
211 20%), the system is probably in a fragmented phase (Saravia & Momo 2017).

212 The  $RS_{max}$  is a useful qualitative index that does not tell us if the system is near or far from the critical  
213 transition; this can be evaluated using the temporal fluctuations. We calculate the fluctuations around the  
214 mean with the absolute values  $\Delta S_{max} = S_{max}(t) - \langle S_{max} \rangle$ , using the proportions of  $RS_{max}$ . To characterize  
215 fluctuations we fitted three empirical distributions: power-law, log-normal, and exponential, using the same  
216 methods described previously. We expect that large fluctuation near a critical point have heavy tails (log-  
217 normal or power-law) and that fluctuations far from a critical point have exponential tails, corresponding  
218 to Gaussian processes (Rooij *et al.* 2013). As the data set spans 15 years, we do not have enough power to  
219 reliably detect which distribution is better (Clauset *et al.* 2009). To improve this we performed the goodness  
220 of fit test described above for all the distributions. We generated animated maps showing the fluctuations  
221 of the two largest patches to aid in the interpretations of the results.

222 A robust way to detect if the system is near a critical transition is to analyze the increase in variance of  
223 the density (Benedetti-Cecchi *et al.* 2015). It has been demonstrated that the variance increase in density  
224 appears when the system is very close to the transition (Corrado *et al.* 2014), thus practically it does  
225 not constitute an early warning indicator. An alternative is to analyze the variance of the fluctuations of  
226 the largest patch  $\Delta S_{max}$ : the maximum is attained at the critical point but a significant increase occurs  
227 well before the system reaches the critical point (Corrado *et al.* 2014). In addition, before the critical  
228 fragmentation, the skewness of the distribution of  $\Delta S_{max}$  should be negative, implying that fluctuations  
229 below the average are more frequent. We characterized the increase in the variance using quantile regression:  
230 if variance is increasing the slopes of upper or/and lower quartiles should be positive or negative.

231 All statistical analyses were performed using the GNU R version 3.3.0 (R Core Team 2015), using code  
232 provided by Cosma R. Shalizi for fitting the power law with exponential cutoff model and the poweRlaw  
233 package (Gillespie 2015) for fitting the other distributions. For the generalized least squares linear model we  
234 used the R function gls from package nlme (Pinheiro *et al.* 2016); and we fitted quantile regressions using  
235 the R package quantreg (Koenker 2016). Image processing was done in MATLAB r2015b (The Mathworks  
236 Inc.). The complete source code for image processing and statistical analysis, and the patch size data files  
237 are available at figshare <http://dx.doi.org/10.6084/m9.figshare.4263905>.

## 238 Results

239 The figure 1 shows an example of the distribution of the biggest 200 patches for years 2000 and 2014, this  
240 distribution is highly variable, but the biggest patch usually maintains its place. Sometimes the biggest  
241 patch breaks and then big fluctuations in its size are observed, as we will analyze below. Smaller patches

242 can merge or break more easily so they enter or leave the list of 200, and this is why there is a color change  
243 across years.

244 The power law distribution was selected as the best model in 92% of the cases (Appendix S4, Figure S7).  
245 In a small number of cases (1%) the power law with exponential cutoff was selected, but the value of the  
246 parameter  $\alpha$  was similar by  $\pm 0.02$  to the pure power law. Additionally the patch size where the exponential  
247 tail begins is very large, thus we used the power law parameters for this cases (See Appendix S4, Figure S2,  
248 region EUAS3). In finite-size systems the favored model should be the power law with exponential cutoff,  
249 because the power-law tails are truncated to the size of the system (Stauffer & Aharony 1994). Here the  
250 regions are so large that the cutoff is practically not observed.

251 There is only one region that did not follow a power law: Eurasia mainland, which showed a log-normal  
252 distribution, representing 7% of the cases. The log-normal and power law are both heavy tailed distributions  
253 and difficult to distinguish, but in this case Akaike weights have very high values for log-normal (near 1),  
254 meaning that this is the only possible model. In addition, the goodness of fit tests clearly rejected the power  
255 law model in all cases for this region (Appendix S4, table S1, region EUAS1). In general the goodness of fit  
256 test rejected the power law model in fewer than 10% of cases. In large forest areas like Africa mainland (AF1)  
257 or South America tropical-subtropical (SAST1), larger deviations are expected and the rejections rates are  
258 higher so the proportion is 30% or less (Appendix S4, Table S1).

259 Taking into account the bootstrapped confidence intervals of each power law exponent ( $\alpha$ ) and the temporal  
260 autocorrelation, there were no significant differences between  $\alpha$  for the regions with the biggest (greater than  
261  $10^7 \text{ km}^2$ ) forest areas (Figure 2 and Appendix S4, Figure S8). There were also no differences between these  
262 regions and smaller ones (Appendix S4, Tables S2 & S3), and all the slopes of  $\alpha$  were not different from  
263 0 (Appendix S4, Table S3). This implies a global average  $\alpha = 1.908$ , with a bootstrapped 95% confidence  
264 interval between 1.898 and 1.920.

265 The proportion of the largest patch relative to total forest area  $RS_{max}$  for regions with more than  $10^7 \text{ km}^2$   
266 of forest is shown in figure 3. South America tropical and subtropical (SAST1) and North America (NA1)  
267 have a higher  $RS_{max}$  of more than 60%, and other big regions 40% or less. For regions with less total  
268 forest area (Appendix S4, figure S9 & Table 1), the United Kingdom (EUAS3) has a very low proportion  
269 near 1%, while other regions such as New Guinea (OC2) and Malaysia/Kalimantan (OC3) have a very high  
270 proportion. SEAS2 (Philippines) is a very interesting case because it seems to be under 30% until the year  
271 2005, fluctuates in the range 30-60%, and then stays over 60% (Appendix S4, figure S9).

272 We analyzed the distributions of fluctuations of the largest patch relative to total forest area  $\Delta RS_{max}$

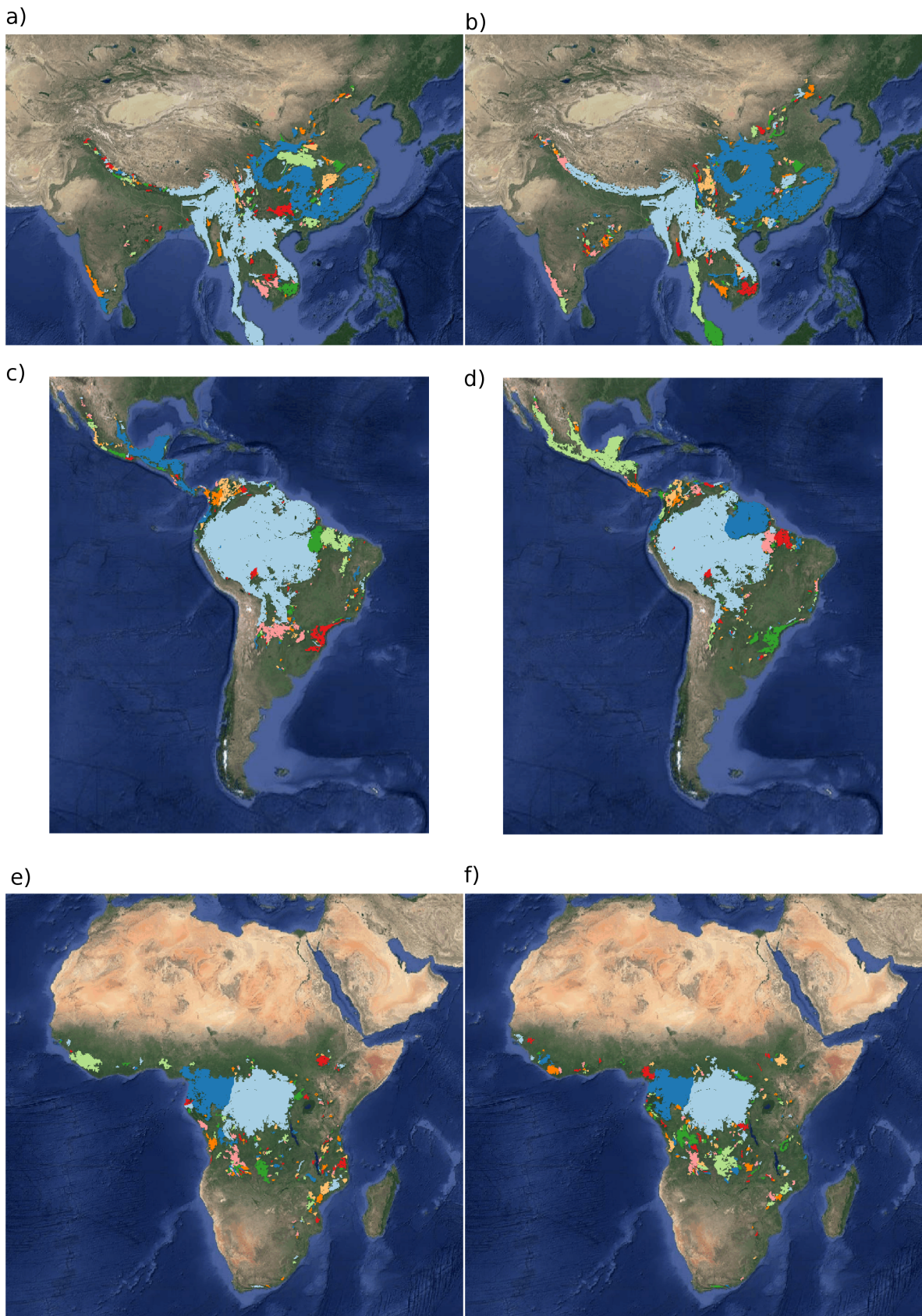


Figure 1: Forest patch distributions for continental regions for the years 2000 and 2014. The images are the 200 biggest patches, showed at a coarse pixel scale of 2.5 Km. The regions are: a) & b) southeast Asia; c) & d) South America subtropical and tropical and e) & f) Africa mainland, for the years 2000 and 2014 respectively.

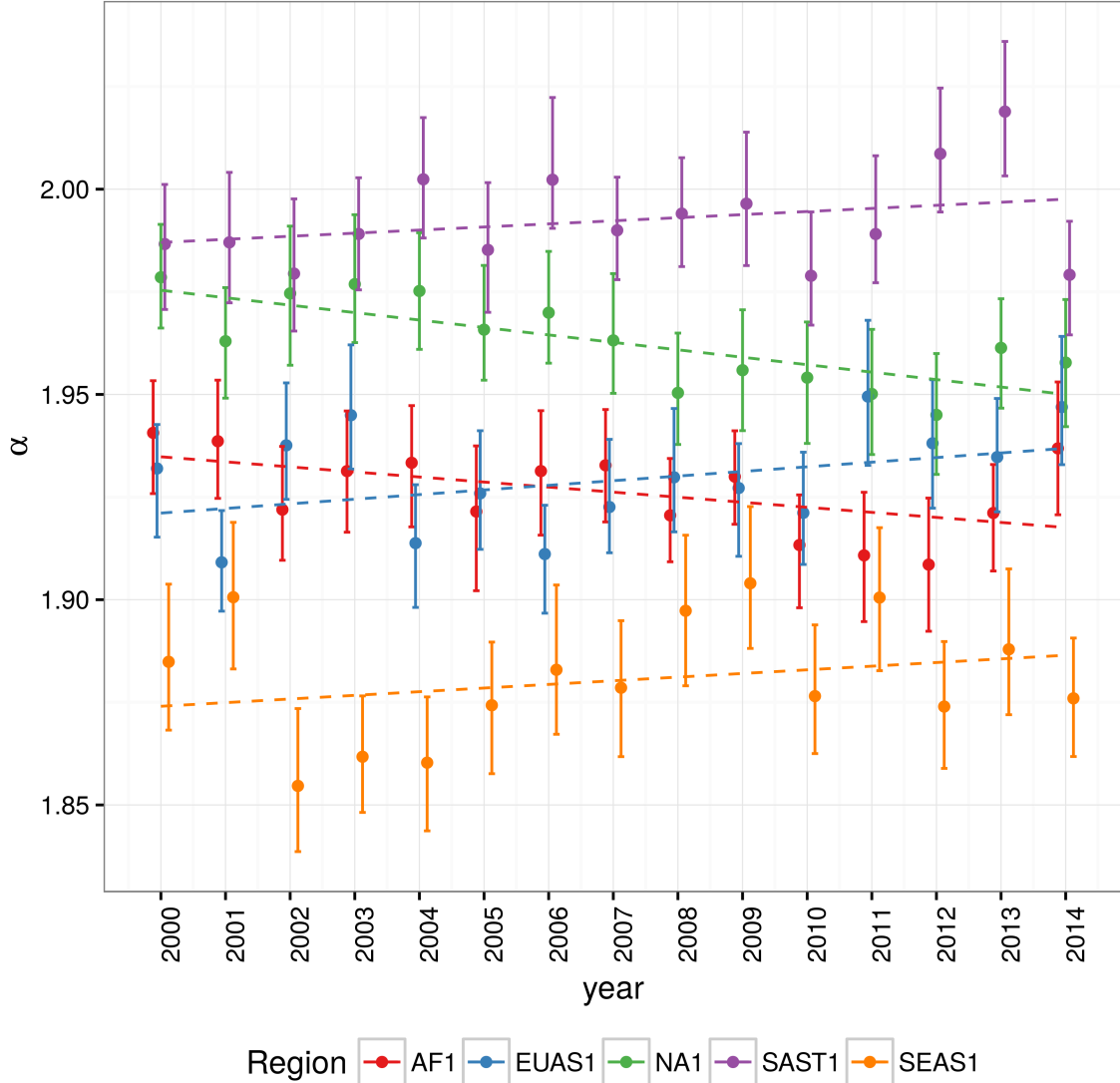


Figure 2: Power law exponents ( $\alpha$ ) of forest patch distributions for regions with total forest area  $> 10^7 \text{ km}^2$ . Dashed horizontal lines are the fitted generalized least squares linear model, with 95% confidence interval error bars estimated by bootstrap resampling. The regions are AF1: Africa mainland, EUAS1: Eurasia mainland, NA1: North America mainland, SAST1: South America subtropical and tropical, SEAS1: Southeast Asia mainland. For EUAS1 the best model is log-normal but the exponents are included here for comparison.

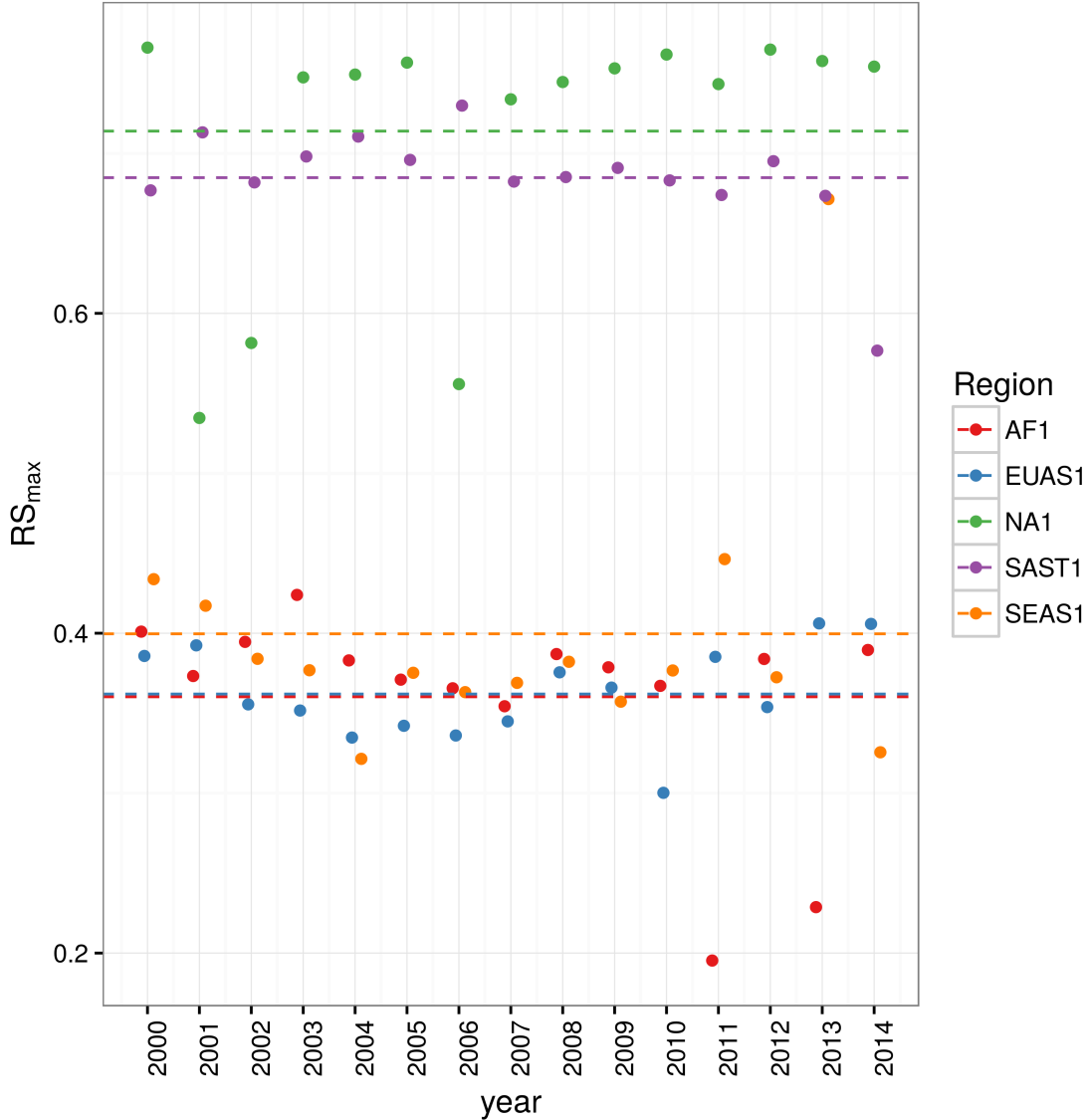


Figure 3: Largest patch proportion relative to total forest area  $RS_{max}$ , for regions with total forest area  $> 10^7 \text{ km}^2$ . Dashed lines are averages across time. The regions are AF1: Africa mainland, EUAS1: Eurasia mainland, NA1: North America mainland, SAST1: South America tropical and subtropical, SEAS1: Southeast Asia mainland.

and the fluctuations of the largest patch  $\Delta S_{max}$ . The model selection for  $\Delta S_{max}$  resulted in power law distributions for all regions (Appendix S4, table S6). For  $\Delta RS_{max}$  instead some regions showed exponential distributions: Eurasia mainland (EUAS1), New Guinea (OC2), Malaysia (OC3), New Zealand (OC6, OC8) and Java (OC7), all others were power laws (Appendix S4, Table S7). The goodness of fit test (GOF) did not reject power laws in any case, but neither did it reject the other models except in a few cases; this was due to the small number of observations. We only considered fluctuations to follow a power law when this distribution was selected for both absolute and relative fluctuations.

The animations of the two largest patches (see supplementary data, largest patch gif animations) qualitatively shows the nature of fluctuations and if the state of the forest is connected or not. If the largest patch is always the same patch over time, the forest is probably not fragmented; this happens for regions with  $RS_{max}$  of more than 40% such as AF2 (Madagascar), NA1 (North America), and OC3 (Malaysia). In the regions with  $RS_{max}$  between 40% and 30% the identity of the largest patch could change or stay the same in time. For OC7 (Java) the largest patch changes and for AF1 (Africa mainland) it stays the same. Only for EUAS1 (Eurasia mainland) we observed that the two largest patches are always the same, implying that this region is probably composed of two independent domains and should be divided in further studies. The regions with  $RS_{max}$  less than 25%: SAST2 (Cuba) and EUAS3 (United Kingdom), the largest patch always changes reflecting their fragmented state. In the case of SEAS2 (Philippines) a transition is observed, with the identity of the largest patch first variable, and then constant after 2010.

The results of quantile regressions are identical for  $\Delta RS_{max}$  and  $\Delta S_{max}$  (Appendix S4, table S4). Among the biggest regions, Africa (AF1) has upper and lower quantiles with significantly negative slopes, but the lower quantile slope is lower, implying that negative fluctuations and variance are increasing (Figure 4). Eurasia mainland (EUAS1) has only the upper quantile significant with a positive slope, suggesting an increase in the variance. North America mainland (NA1) exhibits a significant lower quantile with positive slope, implying decreasing variance. Finally, for mainland Australia, all quantiles are significant, and the slope of the lower quantiles is greater than the upper ones, showing that variance is decreasing (Appendix S4, figure S10). These results are summarized in Table 1.

The conditions that indicate that a region is near a critical fragmentation threshold are that patch size distributions follow a power law; temporal  $\Delta RS_{max}$  fluctuations follow a power law; variance of  $\Delta RS_{max}$  is increasing in time; and skewness is negative. All these conditions were true only for Africa mainland (AF1) and South America tropical & subtropical (SAST1).

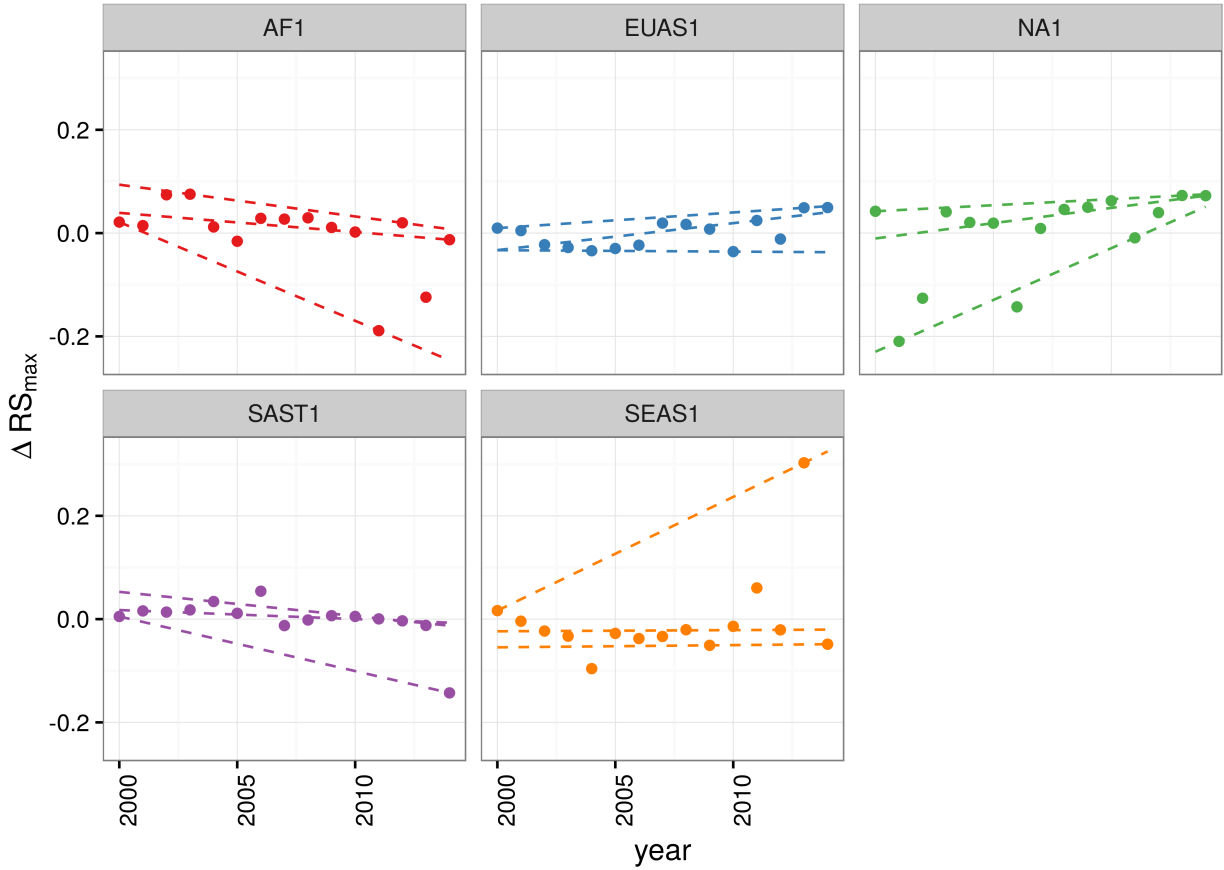


Figure 4: Largest patch fluctuations for regions with total forest area  $> 10^7 \text{ km}^2$  across years. The patch sizes are relative to the total forest area of the same year. Dashed lines are 90%, 50% and 10% quantile regressions, to show if fluctuations were increasing. The regions are AF1: Africa mainland, EUAS1: Eurasia mainland, NA1: North America mainland, SAST1: South America tropical and subtropical, SEAS1: Southeast Asia mainland.

Table 1: Regions and indicators of closeness to a critical fragmentation threshold. Where,  $RS_{max}$  is the largest patch divided by the total forest area,  $\Delta RS_{max}$  are the fluctuations of  $RS_{max}$  around the mean, skewness was calculated for  $RS_{max}$  and the increase or decrease in the variance was estimated using quantile regressions, NS means the results were non-significant. The conditions that determine the closeness to a threshold are: power law distributions in patch sizes and  $\Delta RS_{max}$ ; increasing variance of  $\Delta RS_{max}$  and negative skewness.

Region	Description	Average	Patch Size			
		$RS_{max}$	Distrib	$\Delta RS_{max}$	Distrib.	Skewness
AF1	Africa mainland	0.36	Power	Power	-1.8630	Increase
AF2	Madagascar	0.65	Power	Power	-0.2478	NS
EUAS1	Eurasia, mainland	0.36	LogNormal	Exp	0.4016	Increase
EUAS2	Japan	0.94	Power	Power	0.0255	NS
EUAS3	United Kingdom	0.07	Power	Power	2.1330	NS
NA1	North America, mainland	0.71	Power	Power	-1.5690	Decrease
NA5	Newfoundland	0.87	Power	Power	-0.7411	NS
OC1	Australia, Mainland	0.28	Power	Power	0.0685	Decrease
OC2	New Guinea	0.97	Power	Exp	0.1321	Decrease
OC3	Malaysia/Kalimantan	0.97	Power	Exp	-0.9633	NS
OC4	Sumatra	0.92	Power	Power	1.3150	Increase
OC5	Sulawesi	0.87	Power	Power	-0.3863	NS
OC6	New Zealand South Island	0.76	Power	Exp	-0.6683	NS
OC7	Java	0.38	Power	Exp	-0.1948	NS
OC8	New Zealand North Island	0.75	Power	Exp	0.2940	NS
SAST1	South America, Tropical and subtropical forest up to Mexico	0.68	Power	Power	-2.7760	Increase
SAST2	Cuba	0.21	Power	Power	0.2751	NS
SAT1	South America, Temperate forest	0.60	Power	Power	-1.5070	Decrease
SEAS1	Southeast Asia, Mainland	0.40	Power	Power	3.0030	NS
SEAS2	Philippines	0.54	Power	Power	0.3113	Increase

## 303 Discussion

304 We found that the forest patch distribution of most regions of the world followed power laws spanning  
 305 seven orders of magnitude. These include tropical rainforest, boreal and temperate forest. Power laws have  
 306 previously been found for several kinds of vegetation, but never at global scales as in this study. Interestingly,  
 307 Eurasia does not follow a power law, but it is a geographically extended region, consisting of different domains  
 308 (as we observed in the largest patch animations, see supplementary data). It is known that the union of two  
 309 independent power law distributions produces a lognormal distribution (Rooij *et al.* 2013). Future studies  
 310 should split this region into two or more new regions, and test if the underlying distributions are power laws.  
 311 Several mechanisms have been proposed for the emergence of power laws in forest: the first is related self  
 312 organized criticality (SOC), when the system is driven by its internal dynamics to a critical state; this has

been suggested mainly for fire-driven forests (Zinck & Grimm 2009; Hantson, Pueyo & Chuvieco 2015). Real ecosystems do not seem to meet the requirements of SOC dynamics (Sole, Alonso & Mckane 2002; Pueyo *et al.* 2010; McKenzie & Kennedy 2012). A second possible mechanism, suggested by Pueyo *et al.* (2010), is isotropic percolation, when a system is near the critical point power law structures arise. This is equivalent to the random forest model that we explained previously, and requires the tuning of an external environmental condition to carry the system to this point. We did not expect forest growth to be a random process at local scales, but it is possible that combinations of factors cancel out to produce seemingly random forest dynamics at large scales. If this is the case the power law exponent should be theoretically near  $\alpha = 2.055$ ; this is close but outside the confidence interval we observed (1.898 - 1.920). The third mechanism suggested as the cause of pervasive power laws in patch size distribution is facilitation (Manor & Shnerb 2008; Irvine, Bull & Keeling 2016): a patch surrounded by forest will have a smaller probability of been deforested or degraded than an isolated patch. We hypothesize that models that include facilitation could explain the patterns observed here. The model of Scanlon *et al.* (2007) showed an  $\alpha = 1.34$  which is also different from our results. Another model but with three states (tree/non-tree/degraded), including local facilitation and grazing, was also used to obtain power laws patch distributions without external tuning, and exhibited deviations from power laws at high grazing pressures (Kéfi *et al.* 2007). The values of the power law exponent  $\alpha$  obtained for this model are dependent on the intensity of facilitation, when facilitation is more intense the exponent is higher, but the maximal values they obtained are still lower than the ones we observed. The interesting point is that the value of the exponent is dependent on the parameters, and thus the observed  $\alpha$  might be obtained with some parameter combination.

It has been suggested that a combination of spatial and temporal indicators could more reliably detect critical transitions (Kéfi *et al.* 2014). In this study, we combined five criteria to detect the closeness to a fragmentation threshold. Two of them were spatial: the forest patch size distribution, and the proportion of the largest patch relative to total forest area ( $RS_{max}$ ). The other three were the distribution of temporal fluctuations in the largest patch size, the trend in the variance, and the skewness of the fluctuations. Each one of these is not a strong individual predictor, but their combination gives us an increased degree of confidence about the system being close to a critical transition.

We found that only the tropical forest of Africa and South America met all five criteria, and thus seem to be near a critical fragmentation threshold. This confirms previous studies that point to these two tropical areas as the most affected by deforestation (Hansen *et al.* 2013). Africa seems to be more affected, because the proportion of the largest patch relative to total forest area ( $RS_{max}$ ) is near 30%, which could indicate that the transition is already started. Moreover, this region was estimated to be potentially bistable, with

345 the possibility to completely transform into a savanna (Staver, Archibald & Levin 2011). The main driver  
346 of deforestation in this area was smallholder farming.

347 The region of South America tropical forest has a  $RS_{max}$  of more than 60%, suggesting that the fragmentation  
348 transition is approaching but not yet started. In this region, a striking decline in deforestation rates has  
349 been observed in Brasil, which hosts most of the biggest forest patch, but deforestation rates have continued  
350 to increase in surrounding countries (Argentina, Paraguay, Bolivia, Colombia, Peru) thus the region is still  
351 at a high risk.

352 The monitoring of biggest patches is also important because they contain most of the intact forest landscapes  
353 defined by Potapov *et al.* (2008), thus a relatively simple way to evaluate the risk in these areas is to use  
354  $RS_{max}$  index. The analysis of  $RS_{max}$  reveals that the island of Philippines (SEAS2) seems to be an example  
355 of a critical transition from an unconnected to a connected state, the early warning signals can be qualitatively  
356 observed: a big fluctuation in a negative direction precedes the transition and then  $RS_{max}$  stabilizes over  
357 60% (Figure S9). In addition, there was a total loss of forest cover of 1.9% from year 2000 to 2012 (Hansen *et*  
358 *al.* 2013) and deforestation rates were not substantially reduced in 1990-2014; this could be the results of an  
359 active intervention of the government promoting conservation and rehabilitation of protected areas, ban of  
360 logging old-growth forest, reforestation of barren areas, community-based forestry activities, and sustainable  
361 forest management in the country's production forest (Lasco *et al.* 2008). This confirms that the early  
362 warning indicators proposed here work in the correct direction.

363 The region of Southeast Asia was also one of the most deforested places in the world, but was not detected  
364 as a region near a fragmentation threshold. This is probably due to the forest conservation and restoration  
365 programs implemented by the Chinese government, which bans logging in natural forests and monitor illegal  
366 harvesting (Viña *et al.* 2016). The MODIS dataset does not detect if native forest is replaced by agroindus-  
367 trial tree plantations like oil palms, that are among the main drivers of deforestation in this area (Malhi *et*  
368 *al.* 2014). To improve the estimation of forest patches, data sets as the MODIS cropland probability and  
369 others about land use, protected areas, forest type, should be incorporated (Hansen *et al.* 2014; Sexton *et*  
370 *al.* 2015).

371 Deforestation and fragmentation are closely related. At low levels of habitat reduction species population  
372 will decline proportionally; this can happen even when the habitat fragments retain connectivity. As habi-  
373 tat reduction continues, the critical threshold is approached and connectivity will have large fluctuations  
374 (Brook *et al.* 2013). This could trigger several negative synergistic effects: populations fluctuations and the  
375 possibility of extinctions will rise, increasing patch isolation and decreasing connectivity (Brook *et al.* 2013).

376 This positive feedback mechanism will be enhanced when the fragmentation threshold is reached, resulting  
377 in the loss of most habitat specialist species at a landscape scale (Pardini *et al.* 2010). Some authors argue  
378 that since species have heterogeneous responses to habitat loss and fragmentation, and biotic dispersal is  
379 limited, the importance of thresholds is restricted to local scales or even that its existence is questionable  
380 (Brook *et al.* 2013). Fragmentation is by definition a local process that at some point produces emergent  
381 phenomena over the entire landscape, even if the area considered is infinite (Oborny, Meszéna & Szabó  
382 2005). In addition, after a region's fragmentation threshold connectivity decreases, there is still a large and  
383 internally well connected patch that can maintain sensitive species (Martensen *et al.* 2012). What is the  
384 time needed for these large patches to become fragmented, and pose a real danger of extinction to a myriad  
385 of sensitive species? If a forest is already in a fragmented state, a second critical transition from forest to  
386 non-forest could happen, this was called the desertification transition (Corrado *et al.* 2014). Considering  
387 the actual trends of habitat loss, and studying the dynamics of non-forest patches—instead of the forest  
388 patches as we did here—the risk of this kind of transition could be estimated. The simple models proposed  
389 previously could also be used to estimate if these thresholds are likely to be continuous and reversible or  
390 discontinuous and often irreversible (Weissmann & Shnerb 2016), and the degree of protection (e.g. using  
391 the set-asides strategy Banks-Leite *et al.* (2014)) than would be necessary to stop this trend.

392 The effectiveness of landscape management is related to the degree of fragmentation, and the criteria to direct  
393 reforestation efforts could be focused on regions near a transition (Oborny *et al.* 2007). Regions that are in  
394 an unconnected state require large efforts to recover a connected state, but regions that are near a transition  
395 could be easily pushed to a connected state; feedbacks due to facilitation mechanisms might help to maintain  
396 this state. Crossing the fragmentation critical point in forests could have negative effects on biodiversity and  
397 ecosystem services (Haddad *et al.* 2015), but it could also produce feedback loops at different levels of the  
398 biological hierarchy. This means that a critical transition produced at a continental scale could have effects  
399 at the level of communities, food webs, populations, phenotypes and genotypes (Barnosky *et al.* 2012). All  
400 these effects interact with climate change, thus there is a potential production of cascading effects that could  
401 lead to a global collapse. Therefore, even if critical thresholds are reached only in some forest regions at a  
402 continental scale, a cascading effect with global consequences could still be produced, and may contribute to  
403 reach a planetary tipping point (Reyer *et al.* 2015). The risk of such event will be higher if the dynamics of  
404 separate continental regions are coupled (Lenton & Williams 2013). Using the time series obtained in this  
405 work the coupling of the continental could be further investigated. It has been proposed that to assess the  
406 probability of a global scale shift, different small scale ecosystems should be studied in parallel (Barnosky *et*  
407 *al.* 2012). As forest comprises a major proportion of such ecosystems, we think that the transition of forests

408 could be used as a proxy for all the underling changes and as a successful predictor of a planetary tipping  
409 point.

410 **Supporting information**

411 **Appendix**

412 *Table S1:* Proportion of Power law models not rejected by the goodness of fit test at  $p \leq 0.05$  level.

413 *Table S2:* Generalized least squares fit by maximizing the restricted log-likelihood.

414 *Table S3:* Simultaneous Tests for General Linear Hypotheses of the power law exponent.

415 *Table S4:* Quantile regressions of the proportion of largest patch area vs year.

416 *Table S5:* Unbiased estimation of skewness for absolute largest patch fluctuations and relative fluctuations.

417 *Table S6:* Model selection using Akaike criterion for largest patch fluctuations in absolute values

418 *Table S7:* Model selection for fluctuation of largest patch in relative to total forest area.

419 *Figure S1:* Regions for Africa (AF), 1 Mainland, 2 Madagascar.

420 *Figure S2:* Regions for Eurasia (EUAS), 1 Mainland, 2 Japan, 3 United Kingdom.

421 *Figure S3:* Regions for North America (NA), 1 Mainland, 5 Newfoundland.

422 *Figure S4:* Regions for Australia and islands (OC), 1 Australia mainland; 2 New Guinea; 3 Malaysia/Kalimantan;  
423 4 Sumatra; 5 Sulawesi; 6 New Zealand south island; 7 Java; 8 New Zealand north island.

424 *Figure S5:* Regions for South America, SAST1 Tropical and subtropical forest up to Mexico; SAST2 Cuba;

425 SAT1 South America, Temperate forest.

426 *Figure S6:* Regions for Southeast Asia (SEAS), 1 Mainland; 2 Philippines.

427 *Figure S7:* Proportion of best models selected for patch size distributions using the Akaike criterion.

428 *Figure S8:* Power law exponents for forest patch distributions by year.

429 *Figure S9:* Largest patch proportion relative to total forest area  $RS_{max}$ , for regions with total forest area  
430 less than  $10^7 \text{ km}^2$ .

431 *Figure S10:* Fluctuations of largest patch for regions with total forest area less than  $10^7 \text{ km}^2$ . The patch  
432 sizes are relativized to the total forest area for that year.

433 **Data Accessibility**

434 Csv text file with model fits for patch size distribution, and model selection for all the regions; Gif Animations  
435 of a forest model percolation; Gif animations of largest patches; patch size files for all years and regions  
436 used here; and all the R and Matlab scripts are available at figshare <http://dx.doi.org/10.6084/m9.figshare.4263905>.

438 **Acknowledgments**

439 LAS and SRD are grateful to the National University of General Sarmiento for financial support. This work  
440 was partially supported by a grant from CONICET (PIO 144-20140100035-CO).

441 **References**

- 442 Allington, G.R.H. & Valone, T.J. (2010) Reversal of desertification: The role of physical and chemical soil  
443 properties. *Journal of Arid Environments*, **74**, 973–977.
- 444 Banks-Leite, C., Pardini, R., Tambosi, L.R., Pearse, W.D., Bueno, A.A., Bruscagin, R.T., Condez, T.H.,  
445 Dixo, M., Igari, A.T., Martensen, A.C. & Metzger, J.P. (2014) Using ecological thresholds to evaluate the  
446 costs and benefits of set-asides in a biodiversity hotspot. *Science*, **345**, 1041–1045.
- 447 Barnosky, A.D., Hadly, E.A., Bascompte, J., Berlow, E.L., Brown, J.H., Fortelius, M., Getz, W.M., Harte, J.,  
448 Hastings, A., Marquet, P.A., Martinez, N.D., Mooers, A., Roopnarine, P., Vermeij, G., Williams, J.W., Gille-  
449 spie, R., Kitzes, J., Marshall, C., Matzke, N., Mindell, D.P., Revilla, E. & Smith, A.B. (2012) Approaching  
450 a state shift in Earth’s biosphere. *Nature*, **486**, 52–58.
- 451 Bascompte, J. & Solé, R.V. (1996) Habitat fragmentation and extinction threholds in spatially explicit  
452 models. *Journal of Animal Ecology*, **65**, 465–473.
- 453 Bazant, M.Z. (2000) Largest cluster in subcritical percolation. *Physical Review E*, **62**, 1660–1669.
- 454 Belward, A.S. (1996) *The IGBP-DIS Global 1 Km Land Cover Data Set “DISCover”: Proposal and Imple-  
455 mentation Plans : Report of the Land Recover Working Group of IGBP-DIS*. IGBP-DIS Office.
- 456 Benedetti-Cecchi, L., Tamburello, L., Maggi, E. & Bulleri, F. (2015) Experimental Perturbations Modify the  
457 Performance of Early Warning Indicators of Regime Shift. *Current biology*, **25**, 1867–1872.
- 458 Bestelmeyer, B.T., Ellison, A.M., Fraser, W.R., Gorman, K.B., Holbrook, S.J., Laney, C.M., Ohman, M.D.,

- 459 Peters, D.P.C., Pillsbury, F.C., Rassweiler, A., Schmitt, R.J. & Sharma, S. (2011) Analysis of abrupt tran-  
460 sitions in ecological systems. *Ecosphere*, **2**, 129.
- 461 Boettiger, C. & Hastings, A. (2012) Quantifying limits to detection of early warning for critical transitions.  
462 *Journal of The Royal Society Interface*, **9**, 2527–2539.
- 463 Bonan, G.B. (2008) Forests and Climate Change: Forcings, Feedbacks, and the Climate Benefits of Forests.  
464 *Science*, **320**, 1444–1449.
- 465 Botet, R. & Ploszajczak, M. (2004) Correlations in Finite Systems and Their Universal Scaling Properties.  
466 *Nonequilibrium physics at short time scales: Formation of correlations* (ed K. Morawetz), pp. 445–466.  
467 Springer-Verlag, Berlin Heidelberg.
- 468 Brook, B.W., Ellis, E.C., Perring, M.P., Mackay, A.W. & Blomqvist, L. (2013) Does the terrestrial biosphere  
469 have planetary tipping points? *Trends in Ecology & Evolution*.
- 470 Burnham, K. & Anderson, D.R. (2002) *Model selection and multi-model inference: A practical information-*  
471 *theoretic approach*, 2nd. ed. Springer-Verlag, New York.
- 472 Canfield, D.E., Glazer, A.N. & Falkowski, P.G. (2010) The Evolution and Future of Earth's Nitrogen Cycle.  
473 *Science*, **330**, 192–196.
- 474 Carpenter, S.R., Cole, J.J., Pace, M.L., Batt, R., Brock, W.A., Cline, T., Coloso, J., Hodgson, J.R., Kitchell,  
475 J.F., Seekell, D.A., Smith, L. & Weidel, B. (2011) Early Warnings of Regime Shifts: A Whole-Ecosystem  
476 Experiment. *Science*, **332**, 1079–1082.
- 477 Clauset, A., Shalizi, C. & Newman, M. (2009) Power-Law Distributions in Empirical Data. *SIAM Review*,  
478 **51**, 661–703.
- 479 Corrado, R., Cherubini, A.M. & Pennetta, C. (2014) Early warning signals of desertification transitions in  
480 semiarid ecosystems. *Physical Review E - Statistical, Nonlinear, and Soft Matter Physics*, **90**, 62705.
- 481 Crowther, T.W., Glick, H.B., Covey, K.R., Bettigole, C., Maynard, D.S., Thomas, S.M., Smith, J.R., Hintler,  
482 G., Duguid, M.C., Amatulli, G., Tuanmu, M.-N., Jetz, W., Salas, C., Stam, C., Piotto, D., Tavani, R., Green,  
483 S., Bruce, G., Williams, S.J., Wiser, S.K., Huber, M.O., Hengeveld, G.M., Nabuurs, G.-J., Tikhonova, E.,  
484 Borchardt, P., Li, C.-F., Powrie, L.W., Fischer, M., Hemp, A., Homeier, J., Cho, P., Vibrans, A.C., Umunay,  
485 P.M., Piao, S.L., Rowe, C.W., Ashton, M.S., Crane, P.R. & Bradford, M.A. (2015) Mapping tree density at  
486 a global scale. *Nature*, **525**, 201–205.
- 487 Dai, L., Vorselen, D., Korolev, K.S. & Gore, J. (2012) Generic Indicators for Loss of Resilience Before a

- 488 Tipping Point Leading to Population Collapse. *Science*, **336**, 1175–1177.
- 489 DiMiceli, C., Carroll, M., Sohlberg, R., Huang, C., Hansen, M. & Townshend, J. (2015) Annual Global  
490 Automated MODIS Vegetation Continuous Fields (MOD44B) at 250 m Spatial Resolution for Data Years  
491 Beginning Day 65, 2000 - 2014, Collection 051 Percent Tree Cover, University of Maryland, College Park,  
492 MD, USA.
- 493 Drake, J.M. & Griffen, B.D. (2010) Early warning signals of extinction in deteriorating environments. *Nature*,  
494 **467**, 456–459.
- 495 Efron, B. & Tibshirani, R.J. (1994) *An Introduction to the Bootstrap*. Taylor & Francis, New York.
- 496 Filotas, E., Parrott, L., Burton, P.J., Chazdon, R.L., Coates, K.D., Coll, L., Haeussler, S., Martin, K.,  
497 Nocentini, S., Puettmann, K.J., Putz, F.E., Simard, S.W. & Messier, C. (2014) Viewing forests through the  
498 lens of complex systems science. *Ecosphere*, **5**, 1–23.
- 499 Foley, J.A., Ramankutty, N., Brauman, K.A., Cassidy, E.S., Gerber, J.S., Johnston, M., Mueller, N.D.,  
500 O’Connell, C., Ray, D.K., West, P.C., Balzer, C., Bennett, E.M., Carpenter, S.R., Hill, J., Monfreda, C.,  
501 Polasky, S., Rockström, J., Sheehan, J., Siebert, S., Tilman, D. & Zaks, D.P.M. (2011) Solutions for a  
502 cultivated planet. *Nature*, **478**, 337–342.
- 503 Folke, C., Jansson, Å., Rockström, J., Olsson, P., Carpenter, S.R., Iii, F.S.C., Crépin, A.-S., Daily, G.,  
504 Danell, K., Ebbesson, J., Elmquist, T., Galaz, V., Moberg, F., Nilsson, M., Österblom, H., Ostrom, E.,  
505 Persson, Å., Peterson, G., Polasky, S., Steffen, W., Walker, B. & Westley, F. (2011) Reconnecting to the  
506 Biosphere. *AMBIO*, **40**, 719–738.
- 507 Fung, T., O’Dwyer, J.P., Rahman, K.A., Fletcher, C.D. & Chisholm, R.A. (2016) Reproducing static and  
508 dynamic biodiversity patterns in tropical forests: the critical role of environmental variance. *Ecology*, **97**,  
509 1207–1217.
- 510 Gardner, R.H. & Urban, D.L. (2007) Neutral models for testing landscape hypotheses. *Landscape Ecology*,  
511 **22**, 15–29.
- 512 Gastner, M.T., Oborny, B., Zimmermann, D.K. & Pruessner, G. (2009) Transition from Connected to Frag-  
513 mented Vegetation across an Environmental Gradient: Scaling Laws in Ecotone Geometry. *The American  
514 Naturalist*, **174**, E23–E39.
- 515 Gillespie, C.S. (2015) Fitting Heavy Tailed Distributions: The poweRlaw Package. *Journal of Statistical*

- 516 *Software*, **64**, 1–16.
- 517 Gilman, S.E., Urban, M.C., Tewksbury, J., Gilchrist, G.W. & Holt, R.D. (2010) A framework for community  
518 interactions under climate change. *Trends in Ecology & Evolution*, **25**, 325–331.
- 519 Goldstein, M.L., Morris, S.A. & Yen, G.G. (2004) Problems with fitting to the power-law distribution. *The  
520 European Physical Journal B - Condensed Matter and Complex Systems*, **41**, 255–258.
- 521 Haddad, N.M., Brudvig, L.a., Clobert, J., Davies, K.F., Gonzalez, A., Holt, R.D., Lovejoy, T.E., Sexton,  
522 J.O., Austin, M.P., Collins, C.D., Cook, W.M., Damschen, E.I., Ewers, R.M., Foster, B.L., Jenkins, C.N.,  
523 King, a.J., Laurance, W.F., Levey, D.J., Margules, C.R., Melbourne, B.a., Nicholls, a.O., Orrock, J.L.,  
524 Song, D.-X. & Townshend, J.R. (2015) Habitat fragmentation and its lasting impact on Earth's ecosystems.  
525 *Science Advances*, **1**, 1–9.
- 526 Hansen, M., Potapov, P., Margono, B., Stehman, S., Turubanova, S. & Tyukavina, A. (2014) Response to  
527 Comment on “High-resolution global maps of 21st-century forest cover change”. *Science*, **344**, 981.
- 528 Hansen, M.C., Potapov, P.V., Moore, R., Hancher, M., Turubanova, S.A., Tyukavina, A., Thau, D., Stehman,  
529 S.V., Goetz, S.J., Loveland, T.R., Kommareddy, A., Egorov, A., Chini, L., Justice, C.O. & Townshend, J.R.G.  
530 (2013) High-Resolution Global Maps of 21st-Century Forest Cover Change. *Science*, **342**, 850–853.
- 531 Hantson, S., Pueyo, S. & Chuvieco, E. (2015) Global fire size distribution is driven by human impact and  
532 climate. *Global Ecology and Biogeography*, **24**, 77–86.
- 533 Harris, T.E. (1974) Contact interactions on a lattice. *The Annals of Probability*, **2**, 969–988.
- 534 Hastings, A. & Wysham, D.B. (2010) Regime shifts in ecological systems can occur with no warning. *Ecology  
Letters*, **13**, 464–472.
- 536 He, F. & Hubbell, S. (2003) Percolation Theory for the Distribution and Abundance of Species. *Physical  
Review Letters*, **91**, 198103.
- 538 Hinrichsen, H. (2000) Non-equilibrium critical phenomena and phase transitions into absorbing states. *Advances in Physics*, **49**, 815–958.
- 540 Irvine, M.A., Bull, J.C. & Keeling, M.J. (2016) Aggregation dynamics explain vegetation patch-size distri-  
541 butions. *Theoretical Population Biology*, **108**, 70–74.
- 542 Keitt, T.H., Urban, D.L. & Milne, B.T. (1997) Detecting critical scales in fragmented landscapes. *Conser-  
543 vation Ecology*, **1**, 4.
- 544 Kéfi, S., Guttal, V., Brock, W.A., Carpenter, S.R., Ellison, A.M., Livina, V.N., Seekell, D.A., Scheffer, M.,

- 545 Nes, E.H. van & Dakos, V. (2014) Early Warning Signals of Ecological Transitions: Methods for Spatial  
546 Patterns. *PLoS ONE*, **9**, e92097.
- 547 Kéfi, S., Rietkerk, M., Alados, C.L., Pueyo, Y., Papanastasis, V.P., ElAich, A. & Ruiter, P.C. de. (2007)  
548 Spatial vegetation patterns and imminent desertification in Mediterranean arid ecosystems. *Nature*, **449**,  
549 213–217.
- 550 Kitzberger, T., Aráoz, E., Gowda, J.H., Mermoz, M. & Morales, J.M. (2012) Decreases in Fire Spread Prob-  
551 ability with Forest Age Promotes Alternative Community States, Reduced Resilience to Climate Variability  
552 and Large Fire Regime Shifts. *Ecosystems*, **15**, 97–112.
- 553 Klaus, A., Yu, S. & Plenz, D. (2011) Statistical analyses support power law distributions found in neuronal  
554 avalanches. (ed M Zochowski). *PloS one*, **6**, e19779.
- 555 Koenker, R. (2016) quantreg: Quantile Regression.
- 556 Lasco, R.D., Pulhin, F.B., Cruz, R.V.O., Pulhin, J.M., Roy, S.S.N. & Sanchez, P.A.J. (2008) Forest responses  
557 to changing rainfall in the Philippines. *Climate change and vulnerability* (eds N. Leary, C. Conde & J.  
558 Kulkarni), pp. 49–66. Earthscan, London.
- 559 Leibold, M.A. & Norberg, J. (2004) Biodiversity in metacommunities: Plankton as complex adaptive sys-  
560 tems? *Limnology and Oceanography*, **49**, 1278–1289.
- 561 Lenton, T.M. & Williams, H.T.P. (2013) On the origin of planetary-scale tipping points. *Trends in Ecology  
562 & Evolution*, **28**, 380–382.
- 563 Loehle, C., Li, B.-L. & Sundell, R.C. (1996) Forest spread and phase transitions at forest-prairie ecotones in  
564 Kansas, U.S.A. *Landscape Ecology*, **11**, 225–235.
- 565 Malhi, Y., Gardner, T.A., Goldsmith, G.R., Silman, M.R. & Zelazowski, P. (2014) Tropical Forests in the  
566 Anthropocene. *Annual Review of Environment and Resources*, **39**, 125–159.
- 567 Manor, A. & Shnerb, N.M. (2008) Origin of pareto-like spatial distributions in ecosystems. *Physical Review  
568 Letters*, **101**, 268104.
- 569 Martensen, A.C., Ribeiro, M.C., Banks-Leite, C., Prado, P.I. & Metzger, J.P. (2012) Associations of Forest  
570 Cover, Fragment Area, and Connectivity with Neotropical Understory Bird Species Richness and Abundance.  
571 *Conservation Biology*, **26**, 1100–1111.
- 572 Martín, P.V., Bonachela, J.A., Levin, S.A. & Muñoz, M.A. (2015) Eluding catastrophic shifts. *Proceedings*

- 573 *of the National Academy of Sciences*, **112**, E1828–E1836.
- 574 McKenzie, D. & Kennedy, M.C. (2012) Power laws reveal phase transitions in landscape controls of fire  
575 regimes. *Nat Commun*, **3**, 726.
- 576 Mitchell, M.G.E., Suarez-Castro, A.F., Martinez-Harms, M., Maron, M., McAlpine, C., Gaston, K.J., Jo-  
577 hansen, K. & Rhodes, J.R. (2015) Reframing landscape fragmentation's effects on ecosystem services. *Trends  
578 in Ecology & Evolution*, **30**, 190–198.
- 579 Naito, A.T. & Cairns, D.M. (2015) Patterns of shrub expansion in Alaskan arctic river corridors suggest  
580 phase transition. *Ecology and Evolution*, **5**, 87–101.
- 581 Oborny, B., Meszéna, G. & Szabó, G. (2005) Dynamics of Populations on the Verge of Extinction. *Oikos*,  
582 **109**, 291–296.
- 583 Oborny, B., Szabó, G. & Meszéna, G. (2007) Survival of species in patchy landscapes: percolation in space  
584 and time. *Scaling biodiversity*, pp. 409–440. Cambridge University Press.
- 585 Ochoa-Quintero, J.M., Gardner, T.A., Rosa, I., de Barros Ferraz, S.F. & Sutherland, W.J. (2015) Thresholds  
586 of species loss in Amazonian deforestation frontier landscapes. *Conservation Biology*, **29**, 440–451.
- 587 Ódor, G. (2004) Universality classes in nonequilibrium lattice systems. *Reviews of Modern Physics*, **76**,  
588 663–724.
- 589 Pardini, R., Bueno, A. de A., Gardner, T.A., Prado, P.I. & Metzger, J.P. (2010) Beyond the Fragmentation  
590 Threshold Hypothesis: Regime Shifts in Biodiversity Across Fragmented Landscapes. *PLoS ONE*, **5**, e13666.
- 591 Pinheiro, J., Bates, D., DebRoy, S., Sarkar, D. & R Core Team. (2016) nlme: Linear and Nonlinear Mixed  
592 Effects Models.
- 593 Potapov, P., Yaroshenko, A., Turubanova, S., Dubinin, M., Laestadius, L., Thies, C., Aksenov, D., Egorov,  
594 A., Yesipova, Y., Glushkov, I., Karpachevskiy, M., Kostikova, A., Manisha, A., Tsybikova, E. & Zhuravleva,  
595 I. (2008) Mapping the world's intact forest landscapes by remote sensing. *Ecology and Society*, **13**.
- 596 Pueyo, S., de Alencastro Graça, P.M.L., Barbosa, R.I., Cots, R., Cardona, E. & Fearnside, P.M. (2010)  
597 Testing for criticality in ecosystem dynamics: the case of Amazonian rainforest and savanna fire. *Ecology  
598 Letters*, **13**, 793–802.
- 599 R Core Team. (2015) R: A Language and Environment for Statistical Computing.
- 600 Reyer, C.P.O., Rammig, A., Brouwers, N. & Langerwisch, F. (2015) Forest resilience, tipping points and

- 601 global change processes. *Journal of Ecology*, **103**, 1–4.
- 602 Rockstrom, J., Steffen, W., Noone, K., Persson, A., Chapin, F.S., Lambin, E.F., Lenton, T.M., Scheffer, M.,  
603 Folke, C., Schellnhuber, H.J., Nykvist, B., Wit, C.A. de, Hughes, T., Leeuw, S. van der, Rodhe, H., Sorlin,  
604 S., Snyder, P.K., Costanza, R., Svedin, U., Falkenmark, M., Karlberg, L., Corell, R.W., Fabry, V.J., Hansen,  
605 J., Walker, B., Liverman, D., Richardson, K., Crutzen, P. & Foley, J.A. (2009) A safe operating space for  
606 humanity. *Nature*, **461**, 472–475.
- 607 Rooij, M.M.J.W. van, Nash, B., Rajaraman, S. & Holden, J.G. (2013) A Fractal Approach to Dynamic  
608 Inference and Distribution Analysis. *Frontiers in Physiology*, **4**.
- 609 Saravia, L.A. & Momo, F.R. (2017) Biodiversity collapse and early warning indicators in a spatial phase  
610 transition between neutral and niche communities. *PeerJ PrePrints*, **5**, e1589v4.
- 611 Scanlon, T.M., Caylor, K.K., Levin, S.A. & Rodriguez-iturbe, I. (2007) Positive feedbacks promote power-law  
612 clustering of Kalahari vegetation. *Nature*, **449**, 209–212.
- 613 Scheffer, M., Bascompte, J., Brock, W.A., Brovkin, V., Carpenter, S.R., Dakos, V., Held, H., Nes, E.H.V.,  
614 Rietkerk, M. & Sugihara, G. (2009) Early-warning signals for critical transitions. *Nature*, **461**, 53–59.
- 615 Scheffer, M., Walker, B., Carpenter, S., Foley, J. a, Folke, C. & Walker, B. (2001) Catastrophic shifts in  
616 ecosystems. *Nature*, **413**, 591–596.
- 617 Seidler, T.G. & Plotkin, J.B. (2006) Seed Dispersal and Spatial Pattern in Tropical Trees. *PLoS Biology*, **4**,  
618 e344.
- 619 Sexton, J.O., Noojipady, P., Song, X.-P., Feng, M., Song, D.-X., Kim, D.-H., Anand, A., Huang, C., Channan,  
620 S., Pimm, S.L. & Townshend, J.R. (2015) Conservation policy and the measurement of forests. *Nature  
621 Climate Change*, **6**, 192–196.
- 622 Sole, R.V., Alonso, D. & Mckane, A. (2002) Self-organized instability in complex ecosystems. *Philosophical  
623 transactions of the Royal Society of London. Series B, Biological sciences*, **357**, 667–681.
- 624 Solé, R.V. (2011) *Phase Transitions*. Princeton University Press.
- 625 Solé, R.V. & Bascompte, J. (2006) *Self-organization in complex ecosystems*. Princeton University Press, New  
626 Jersey, USA.
- 627 Solé, R.V., Alonso, D. & Saldaña, J. (2004) Habitat fragmentation and biodiversity collapse in neutral

- 628 communities. *Ecological Complexity*, **1**, 65–75.
- 629 Solé, R.V., Bartumeus, F. & Gamarra, J.G.P. (2005) Gap percolation in rainforests. *Oikos*, **110**, 177–185.
- 630 Stauffer, D. & Aharony, A. (1994) *Introduction to Percolation Theory*. Taylor & Francis, London.
- 631 Staver, A.C., Archibald, S. & Levin, S.A. (2011) The Global Extent and Determinants of Savanna and Forest  
632 as Alternative Biome States. *Science*, **334**, 230–232.
- 633 Vasilakopoulos, P. & Marshall, C.T. (2015) Resilience and tipping points of an exploited fish population over  
634 six decades. *Global Change Biology*, **21**, 1834–1847.
- 635 Viña, A., McConnell, W.J., Yang, H., Xu, Z. & Liu, J. (2016) Effects of conservation policy on China's forest  
636 recovery. *Science Advances*, **2**, e1500965.
- 637 Weerman, E.J., Van Belzen, J., Rietkerk, M., Temmerman, S., Kéfi, S., Herman, P.M.J. & Koppell, J.V.  
638 de. (2012) Changes in diatom patch-size distribution and degradation in a spatially self-organized intertidal  
639 mudflat ecosystem. *Ecology*, **93**, 608–618.
- 640 Weissmann, H. & Shnerb, N.M. (2016) Predicting catastrophic shifts. *Journal of Theoretical Biology*, **397**,  
641 128–134.
- 642 Zhang, J.Y., Wang, Y., Zhao, X., Xie, G. & Zhang, T. (2005) Grassland recovery by protection from grazing  
643 in a semi-arid sandy region of northern China. *New Zealand Journal of Agricultural Research*, **48**, 277–284.
- 644 Zinck, R.D. & Grimm, V. (2009) Unifying wildfire models from ecology and statistical physics. *The American  
645 naturalist*, **174**, E170–85.
- 646 Zuur, A.F., Ieno, E.N., Walker, N., Saveliev, A.A. & Smith, G.M. (2009) *Mixed effects models and extensions  
647 in ecology with R*. Springer New York, New York, NY.